JOURNAL OF GEOPHYSICAL RESEARCH, VOL. 87, NO. B13, PAGES 10,983–10,998, DECEMBER 10, 1982

Stratigraphy and Structural Evolution of Southern Mare Serenitatis: A Reinterpretation Based on Apollo Lunar Sounder Experiment Data

VIRGIL L. SHARPTON AND JAMES W. HEAD III

Department of Geological Sciences, Brown University
Providence, Rhode Island 02912

The Apollo Lunar Sounder Experiment (ALSE) detected two subsurface reflecting horizons in southern Mare Serenitatis. These horizons appear to be regolith layers, >2 m thick, which correlate with major stratigraphic boundaries in southeastern Mare Serenitatis. Our analysis differs from previous interpretations and implies that the lower horizon represents the interface between the earliest mare unit (unit I; ~3.8 b.y.) and the modified Serenitatis basin material below. The upper horizon represents the regolith developed by sustained impact bombardment of the unit I surface prior to the emplacement of the intermediate basalts (unit II; ~3.5 b.y.). The latest volcanic episode (unit III; ~3.2 b.y.) resulted in a very thin infilling (<400 m deep) in the southern portion of the basin and was undetected by ALSE. Profiles of the stratigraphic surfaces represented by the ALSE reflecting horizons are reconstructed for three stages in the basin filling history. These reconstructions permit the timing and magnitude of various volcanic and tectonic events within the Serenitatis basin to be assessed. On the basis of comparison with Orientale ring topography, the large subsurface arch is interpreted to be the peak-ring-related topography of the Serenitatis basin. The thickness of mare basalts across the ALSE ground track is highly variable: basalts are <400 m thick above the peak ring, while they reach a maximum thickness of ~2.5 km in the depression between the first and second basin rings. Comparison with Orientale topography suggests that a major increase in basalt thickness of ~6 km may occur ~50 km inside the peak ring. This region was unsampled by the ALSE traverse. Extensive load-induced deformation occurred after the emplacement of unit I (~1.2 km thick, maximum). This loading of the lithosphere resulted in graben formation along the margins of the basin, major downwarping and tilting of the unit I surface, and production of discrete zones of faulting, buckling, and subsidence. Pre-mare topography exerted a strong control over the tectonic patterns in the basin: Topographic highs such as ring structures underwent <400 m of subsidence, whereas intra-ring depressions underwent as much as 1.4 km of downwarping. Although the lithosphere was tectonically most active between the emplacement of units I and III, it continued to respond to the load of units I and II after the emplacement of unit III, as evidenced by ~600 m of postunit III structural relief. The association of all mare ridges transected by the ALSE ground track with distinct offsets or depth changes in the subsurface layering indicates that these surface features are tectonic in origin.

INTRODUCTION

The lithosphere within and around lunar mascon basins has undergone extensive tectonic deformation, as evidenced by the presence of circumferential graben [*Lucchitta and Watkins*, 1978], mare ridges [*Bryan*, 1973; *Muehlberger*, 1974; *Lucchitta*, 1976, 1977; *Sharpton and Head*, 1980, 1981], and post emplacement tilting of mare surfaces [*Muehlberger*, 1974, 1977; *Scott et al.*, 1978]. This deformation appears to be principally a response to the surface load imparted by volcanic infilling [*Kuckes*, 1977; *Melosh*, 1978; *Solomon and Head*, 1979, 1980], although thermal stresses associated either with lunar evolution [*MacDonald*, 1960; *Solomon and Chaiken*, 1976; *Solomon*, 1977; *Solomon and Head*, 1979, 1980] or with the basin-forming impact event [*Bratt et al.*, 1981] may have also influenced tectonism. The nature and extent of this deformation depend on the physical state of the lithosphere as well as the magnitude and distribution of the volcanic load. As the lithosphere deformed, the surfaces of the originally flat-lying basalts developed a topographic expression indicative of the response of the lithosphere to the load. An analysis of topography and surface features developed on, and adjacent to, the mare units of a mascon basin can therefore provide important information concerning the tectonic and volcanic modification of the basin.

The southern portion of Mare Serenitatis has received extensive coverage from the Apollo missions including high-resolution photography, orbital experiments, surface exploration, and returned samples. Consequently, several investigations have been conducted to reconstruct the structural history of this area by analyzing either discrete variations in slope across volcanic unit boundaries [*Howard et al.*, 1973; *Muehlberger*, 1974] or regional topography and sinuous rille gradients [*Muehlberger*, 1977; *Scott et al.*, 1978]. Although the results of these investigations compose a significant contribution toward reconstructing the structural history of Mare Serenitatis, several uncertainties are not fully resolvable by this two dimensional approach including: (1) the thickness of the volcanic fill within Serenitatis, (2) the influence of pre-mare basin morphology on the distribution of mare basalts and on tectonism, and (3) the magnitude and style of deformation which modified the early basalts that now lie buried beneath less deformed mare units [*Howard et al.*, 1973].

In order to resolve some of these uncertainties the model of the geologic history of southern Serenitatis can be expanded to three dimensions by including subsurface information gathered by the Apollo Lunar Sounder Experiment (ALSE). Two subsurface radar reflecting horizons were identified by *Peeples et al.* [1978] extending along the ALSE ground track across the southern portion of the basin (Figure 1). Thought to represent buried regolith layers, these hori-

Paper number 2B1566.
0148-0227/82/002B-1566$05.00

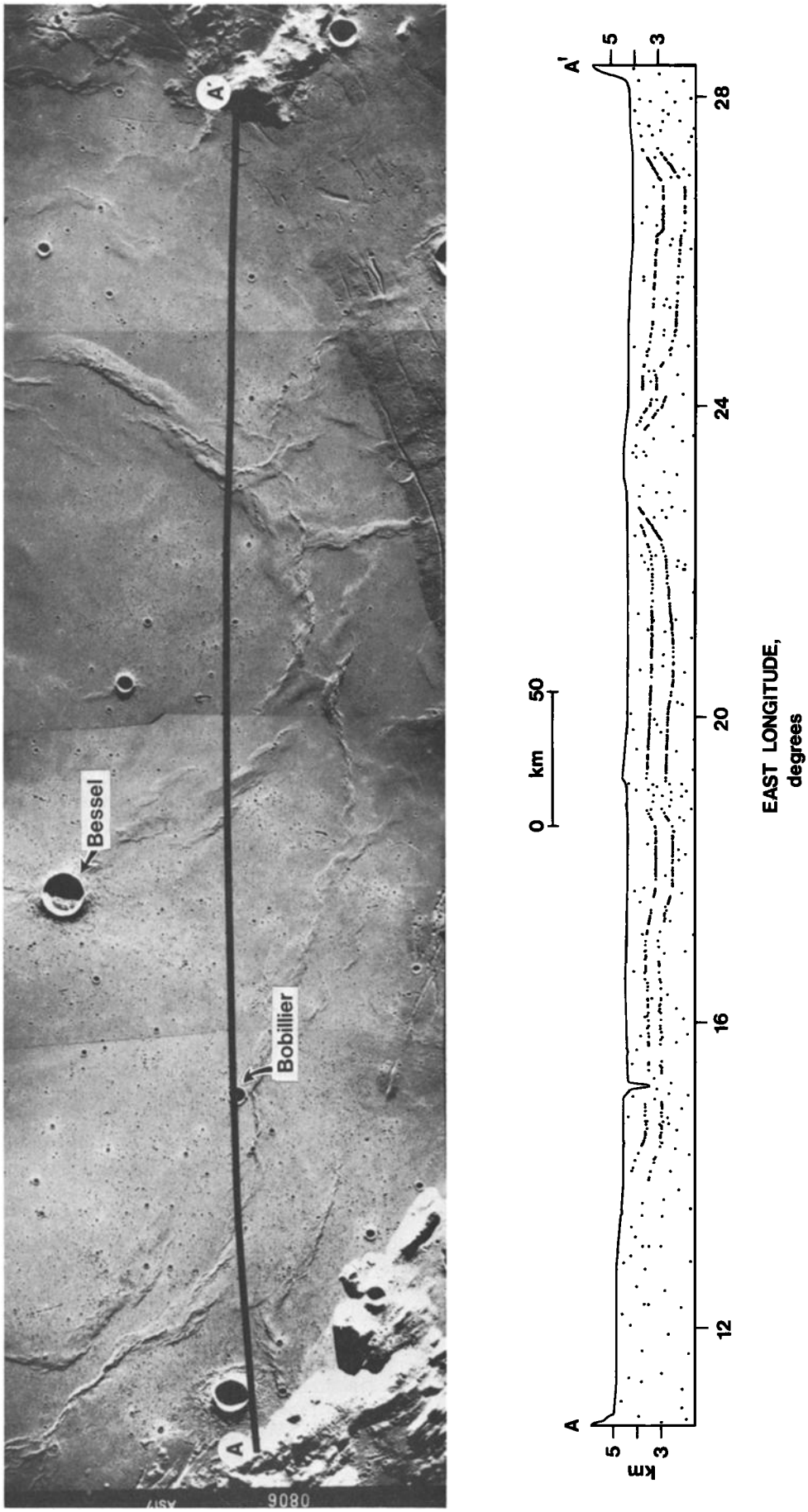

Fig. 1. Photomosaic (Apollo 17 metric −0806, −0804, −0452, −0449) of the southern portion of Mare Serenitatis in the vicinity of the ALSE traverse (denoted by bold line). The cross section shows the ALSE data to the same horizontal scale; vertical scale is in kilometers above an arbitrary zero vertical datum of 1,730,000 m [after *Peeples et al.*, 1978].

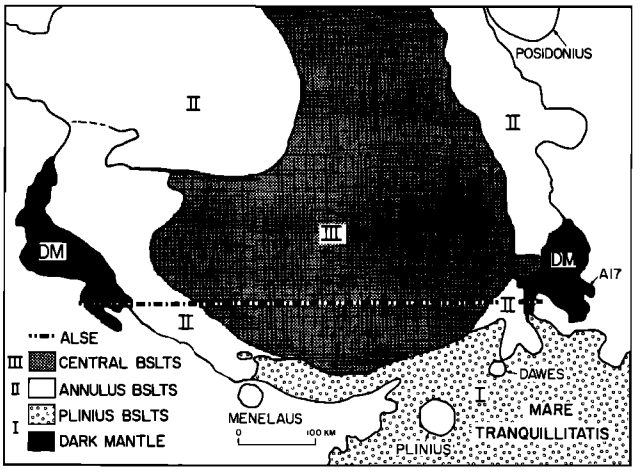

Fig. 2. Geologic sketch map of southern Mare Serenitatis showing the three major mare surface units: I, the oldest; II, intermediate in age; and III, the youngest. Unit I is composed of a dark mantle component (DM) as well as basalts. The bold line denotes the ALSE traverse [after *Solomon and Head*, 1979].

zons appear to mark ancient stratigraphic surfaces buried by later volcanism [*Peeples et al.*, 1978]. The reflecting horizons have been assigned to surface unit boundaries in the southeastern portion of the basin [*May et al.*, 1976; *Maxwell*, 1977, 1978; *Phillips and Maxwell*, 1978].

We have combined geological and geophysical data with subsurface information from the Apollo Lunar Sounder Experiment to reinterpret the subsurface horizons and their stratigraphic correlation. In this paper we present this model and explore the implications pertaining to the geometry of the Serenitatis impact basin, the depth of mare fill, and the structural history of Mare Serenitatis.

THE ALSE RESULTS

Background

The Apollo Lunar Sounder Experiment flown on the Apollo 17 mission included two adjacent east-to-west traverses across Mare Serenitatis. A detailed account of the background, theory, and technique of ALSE is reported by *Phillips et al.* [1973*a*, *b*] and *Porcello et al.* [1974]. ALSE was an orbital wide band coherent radar system operating in three frequency ranges. The deepest subsurface penetration was provided by the HF-1 system operating at 5 MHz. This system, however, did not permit the recognition of subsurface detail less than about 400 m below the surface because of bandwidth limitations [*Peeples et al.*, 1978]. The profile shown in Figure 1 is the result of a technique which correlated returns from both radar traverses across the basin in order to separate the subsurface signal from noise due to surface scatter [*Peeples et al.*, 1978].

The Reflecting Horizons

The two subsurface horizons observed in the ALSE profile (Figure 1) are defined by the linear alignment of closely spaced radar reflectors extending across all but the westernmost portion of the profile. These two horizons have been interpreted as continuous, lateral zones of a high-porosity material such as buried regolith, crater/basin ejecta blankets, or pyroclastic deposits [*May et al.*, 1976; *Peeples et al.*, 1978]. Subsequent analysis [*Maxwell*, 1977; *Phillips and Maxwell*, 1978] has favored a buried regolith model for these horizons. Bandwidth limitations of the HF-1 system require that these regolith layers be greater than 2 m thick to act as reflecting horizons [*Peeples et al.*, 1978].

The ALSE ground track intersects two local dark mantle deposits within Serenitatis (Figure 2): the Taurus-Littrow region to the east [*Lucchitta*, 1973; *Head*, 1974; *Adams et al.*, 1974] and the Sulpicius Gallus region to the west [*Lucchitta and Schmitt*, 1974; *Head*, 1974]. These units are recognized accumulations of pyroclastic material and have distinct surface morphology, albedo, spectral, and radar characteristics [*Lucchitta*, 1973, *Head*, 1974; *Adams et al.*, 1974; *Pieters*, 1978]. However, neither the Haemus mountains nor the Plinius basalts (Figure 2) just to the south of the ALSE traverse exhibit characteristics similar to dark mantle deposits. Furthermore, models of lunar pyroclastic eruptions [*Wilson and Head*, 1981] predict that the volume fraction of material ejected to distances greater than a few tens of kilometers from the source vent is extremely small. Thus a significant basin-wide pyroclastic component to the radar reflecting horizons would require a more-or-less linear array of (now buried) source vents aligned with the ALSE ground track but not extending southward enough to mantle the highlands or Plinius basalts. It seems unlikely, therefore, that the two dark mantle deposits located at the flanks of Mare Serenitatis continue beneath the mare and join to form an uninterrupted, basin-wide pyroclastic unit. The more plausible alternative appears to be that pyroclastics are a significant component only on the local scale; the continuous basin-wide nature of the reflecting horizon calls for a broader scale process.

Regolith, generated by extended exposure to small-scale meteor impacts, is observed on all lunar surfaces [*Oberbeck and Quaide*, 1968]. The length of time a rock surface must remain exposed to impacts to produce a given thickness of regolith depends upon the cratering rate during surface exposure. Even a constant impact flux, however, results in regolith accumulation in which the increase in thickness is

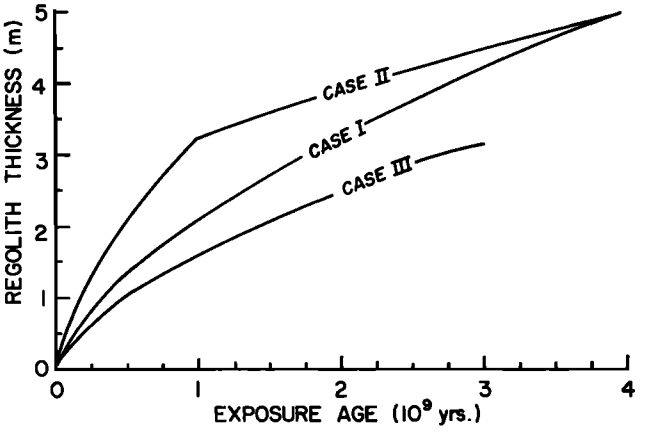

Fig. 3. Regolith growth curves for two lunar mare surfaces: the Apollo 12 site (cases I and II) and Apollo 11 (case III). Cases I and III assume that the present crater distributions at these sites resulted from a constant cratering rate. Case II approximates the effect of an early, higher impact flux by assuming that 50% of the observed craters on the mare surface at Apollo 12 occurred in the first billion years of exposure. This model indicates that it requires a few hundred million years to produce the minimum 2-m regolith required by ALSE resolution limitations. See text for details. Adapted from *Quaide and Oberbeck* [1975].

TABLE 1. Volcanic Stratigraphy of Mare Serenitatis

Volcanic Units *Howard et al.* [1973]	Major Stratigraphic Units: *Howard et al.* [1973]	Major Stratigraphic Units: *Solomon and Head* [1979]	Estimated Age, b.y.
Basalt of Mare Serenitatis	Group C	Unit III	3.0–3.4 [*Neukum et al.*, 1975]
Basalt of southwestern Mare Serenitatis Eastern Ring basalt Basalt near Dawes	Group B	Unit II	~3.5 [*Muehlberger*, 1974]
Basalt of Plinius area Dark mantle of Sulpicius Gallus Formation Dark mantle of Littrow	Group A	Unit I	3.65–3.84 [*Wasserburg et al.*, 1977; *Geiss et al.*, 1977]

The volcanic surfaces listed in column 1 appear to correspond to three major episodes of volcanic activity as shown in columns 2 and 3. The present paper follows the nomenclature of *Solomon and Head* [1979] (column 3). Age estimates for these three major stratigraphic units are presented in column 4.

nonlinear with time [*Quaide and Oberbeck*, 1975; *Hörz*, 1977]. Rapid accumulation occurs early in the exposure history, but as the regolith thickens, it shields the subjacent rock surface from progressively larger impacts, thereby retarding further growth. *Quaide and Oberbeck* [1975] have modeled lunar regolith evolution for two typical mare sites using a Monte Carlo simulation. Figure 3 gives the regolith thickness curves for the three cases examined in this study. Cases I and III assume that the final crater distributions observed at the Apollo 11 (3.65 b.y.) and Apollo 12 (3.2 b.y.) sites, respectively, result from a constant cratering rate. Comparison of cases I and III illustrates that older mare surfaces such as at Apollo 11 produce the required 2 m of regolith in less time than the younger Apollo 12 surface. Considering, however, that the total duration of observed mare volcanism was only $\sim 1 \times 10^9$ years, neither model appears capable of accounting for the subsurface reflecting horizons observed in Figure 1.

Analyses of crater densities on surfaces of various ages [*Hartmann*, 1966, 1970*a*, *b*, 1972] have led to the general consensus that although the lunar cratering rate has remained fairly constant through post-mare time, the early lunar impact flux was significantly higher, decreasing rapidly during the late basin-forming and early mare emplacement stages of the lunar past. That this 'tailing off' in impact flux affected older mare surfaces is apparent from the case I–case III comparison in Figure 3: Case I produces more regolith in any given time interval than does case III. Thus the average crater production rate for case I is greater than the average crater production rate for case III. Since the post 3.2 b.y. average flux was the same for both sites, the elevated density of craters at the older Apollo 11 site must be attributed to an increased flux prior to 3.2 b.y. The effect of this higher impact flux on early regolith development is approximated in Figure 2 by case II, which assumes that for the Apollo 11 site, 50% of the present craters were produced in the first billion years of exposure and the rest at a constant rate since that time. This model, as a first estimate of the effects of the real lunar cratering rate, is capable of producing the required 2 m of regolith in a few hundred million years (Figure 3), within the time constraints imposed by the limited span of mare volcanism. Exposure intervals of less than 10^8 years do not appear sufficient to produce the thickness required for ALSE resolution. The duration of these exposure intervals suggests that the resulting regolith layers should form the boundaries of major volcanic sequences within Mare Serenitatis [*Howard et al.*, 1973]. The ALSE reflecting horizons, therefore, identify the subsurface traces of the boundaries between the major time-stratigraphic units infilling the Serenitatis basin and should be correlatable with unit boundaries at the surface.

STRATIGRAPHY OF SOUTHERN SERENITATIS

Regional Stratigraphy

Thompson et al. [1973] and *Howard et al.* [1973] mapped the areal distribution of the volcanic units within Mare Serenitatis. On the basis of color, albedo, and other remotely measured surface properties, seven individual volcanic units were identified (Table 1, column 1). Subsequent study of vidicon images [*Johnson et al.*, 1975], while suggesting a more complex distribution of surface units, basically supported the previous stratigraphic models. By applying superposition criteria and analyzing surface features and topography, *Howard et al.* [1973] and *Muehlberger* [1974] recognized that these seven volcanic units compose three separate episodes of volcanic activity (Table 1, column 2, and Figure 2). Relative ages of the volcanic units within Mare Serenitatis obtained by regional analysis of crater morphology [*Boyce*, 1976] also imply that emplacement of the mare units was episodic rather than continuous. We follow the convention of *Solomon and Head* [1979] (Table 1, column 3) and denote the oldest, intermediate, and youngest episodes of volcanic activity as unit I, unit II, and unit III, respectively. Determination of absolute ages of the volcanic units infilling Mare Serenitatis is difficult due to the presence of only one sample return site. Isotope ages of mare basalts in Serenitatis exist only for unit I at the Apollo 17 landing site: 3.65–3.84 b.y. [*Wasserburg et al.*, 1977; *Geiss et al.*, 1977] and the associated dark mantle soil component ~3.7 b.y. [*Huneke et al.*, 1973; *Husain and Schaeffer*, 1973; *Tatsumoto et al.*, 1973; *Hintenberger and Weber*, 1973]. *Solomon and Head* [1979] discuss the problems of determining the ages of the unsampled unit II and unit III surfaces and assign an age to unit III of 3.0–3.4 b.y. based on crater-

counting results of *Neukum et al.* [1975] and crater degradation ages of *Boyce* [1976]. Unit II, stratigraphically bounded above by unit III and below by unit I, is assigned an age of ~3.5 b.y. [*Muehlberger*, 1974]. We adopt these age assignments (Table 1, column 4) with the qualifications discussed by *Solomon and Head* [1979].

Southeastern Serenitatis

Interpretations which correlate the reflecting horizons with the boundaries between surface units must be based upon the stratigraphy in the southeastern portion of the basin; the substructure in the western extreme of the profile does not exhibit sufficient resolution to permit extrapolation to the surface. In southeastern Serenitatis, the ALSE profile transects exposed surfaces of all three major volcanic sequences [*Howard et al.*, 1973] as well as the highland massif, Mons Argaeus (A'; Figure 4).

As presented in Figure 4, *Howard et al.* [1973] mapped the boundary between the final volcanic episode (unit III) and the previous sequences (units II and I) to be coincident with the boundary between the light central mare unit and the dark annulus basalts on the margins of the basin. On the basis of crater morphology dating methods, *Maxwell* [1977] interpreted a 10–30 km wide exposure of dark annulus mare (area E basalts in Figure 4) to be the same age as the light central mare shifting the boundary between unit III and unit II (shown by the dashed boundary in Figure 4) eastward by about 30 km. We have reexamined the stratigraphy of this area, employing both high and low sun angle Apollo metric photography as well as relying on Apollo and earth-based remote sensing data and lunar topographic orthophotomaps (LTO's).

Several observations appear to support the original stratigraphic interpretation presented by *Howard et al.* [1973]:

1. A number of fractures and faults deform the surface of area E (Figure 4). At the boundary between area E and the central mare, however, the depressions are truncated. This observation implies that the surface of area E underwent extensional deformation prior to the emplacement of the overlying central mare basalts which are relatively unfractured [*Howard et al.*, 1973].

2. Albedo, color, and remote spectral data [*Howard et al.*, 1973; *Thompson et al.*, 1973; *Johnson et al.*, 1975] suggest a compositional demarcation coincident with the boundary between area E and the central mare.

3. This boundary also serves to separate two distinct zones based on 3.8-cm wavelength characteristics. The central mare is a strong radar reflector, whereas the dark annulus basalts, including area E, are weak reflectors of both polarized and depolarized returns. Since the reflectivity of a mare unit is strongly dependent on the density of the surface material, regolith with relatively few wavelength-sized fragments will have a low reflectivity. It follows then that the reflectivity of mare units of similar composition may be correlatable with the age of the surface: Due to impact-induced comminution older mare surfaces would contain fewer wavelength-sized fragments and thus have a lower reflectivity [*Zisk et al.*, 1973; *Maxwell*, 1977]. On the basis of radar data, therefore, it appears that area E is closer in age to the other dark annulus basalts in this region (unit II) than to the central mare basalts (unit III).

Thus the bulk of the available information suggests that area E is closer in age as well as composition to the other dark annulus basalts rather than the central mare unit. Therefore we follow the stratigraphic interpretation of *Howard et al.* [1973], with the surface boundaries as shown in Figure 4*b*.

CORRELATING THE ALSE DATA WITH SURFACE GEOLOGY

Although limitations of ALSE do not permit the detection of the reflecting horizons in the upper 400 m of the subsurface, the inclination of the eastern end of the horizons provides information about the intersection of these horizons with the surface. The upward projections of the two reflecting horizons intersect the surface in the vicinity of three known stratigraphic boundaries (Figure 4). Thus the correlation of the subsurface reflecting horizons with surface stratigraphic boundaries is subject to different interpretations.

The Original Interpretation

The previous correlation [*May et al.*, 1976; *Maxwell*, 1977; *Phillips and Maxwell*, 1978; *Peeples et al.*, 1978] of the two reflecting horizons with unit boundaries at the surface is presented in Figure 5. This interpretation was accomplished by projecting the subsurface horizons upward along straight lines, continuing the inclination observed at the eastern edge of each horizon. Using this technique, the upper horizon projects to the surface at point D (Figures 4 and 5) where the ALSE ground track intersects the boundary between area E and unit II (Figure 4). As *Maxwell* [1977] interprets area E to be contemporaneous with the central mare basalt, this surface point would be equivalent to the unit III/unit II boundary. The projected upper horizon does not, however, intersect with the boundary between the central mare and the dark annulus basalts (point F) as mapped by *Howard et al.* [1973], as frequently reported [*May et al.*, 1976; *Maxwell*, 1977; *Phillips and Maxwell*, 1978]. The lower horizon would intersect the boundary between unit II and unit I (point C; Figures 4 and 5) if the slope that is apparent on the eastern end of the lower reflector is decreased slightly, as illustrated in Figure 5.

The interpretation summarized above bears reexamination for several reasons:

1. The data presented in the previous section, dealing with the stratigraphy of the southeastern Serenitatis, suggest that the area E basalts (Figure 4) are similar in age and composition to the other unit II basalts. It appears unlikely, therefore, given the slow rate of regolith growth, that 2 m of regolith could develop on the unit II surface before the area E basalts were emplaced. A projection of the upper reflecting horizon to the interface between these two apparent subunits of the same volcanic episode thus seems unjustified.

2. If the upper horizon is to represent the buried portion of the unit II surface, as in this interpretation, it must be projected upward to point D, where the unit II basalts emerge from beneath the area E basalts. In order for the upper horizon to intersect point D the projection path must be a linear continuation of the slope exhibited by the uptilted eastern end of the upper horizon (~4.3°; Figure 5). Any reduction in this slope would force the surface intersection point to the east of point D. Thus the interpretation presented above requires the subsurface continuation of the unit II surface, west of point D, to slope inward at 4.3°. Measurements derived from LTO 42C3 indicate that the unit II surface exposed from point D eastward to point C slopes to

Fig. 4*a*

Fig. 4. Surface units of southeastern Mare Serenitatis. (*a*) Apollo 17 metric photograph 0796 showing area of sketch map to same scale. (*b*) Sketch map illustrating stratigraphic relationships and major surface units discussed in text. A′ is the eastern terminus of the ALSE profile shown in Figure 1; the ALSE traverse intersects the unit I/highlands boundary at B, the unit II/unit I boundary at C, and the unit III/unit II boundary at F. The boundary between the basaltic surface, here labeled area E, and the unit II basalts (dashed line) as mapped by *Maxwell* [1977] intersects the ALSE ground track at D. Bold solid lines define highland-mare boundaries. See text for details.

the west at only ~0.3°. This indicates a discrepancy of ~4° in the unit II surface across point D. A sharp change in slope of this magnitude along a primary depositional surface would require postdepositional folding, with the hinge line of the angular monocline located at point D along the ALSE profile. Folding is precluded, however, because the lower horizon is not similarly folded beneath point D. The lack of a satisfactory explanation for this geometric configuration suggests that the subsurface horizons may correlate with surface boundaries other than those proposed by *May et al.* [1976], *Maxwell* [1977], and *Phillips and Maxwell* [1978].

3. The regional tilt of mare surfaces is a measure of the tectonic deformation the surface has undergone after its emplacement. Thus the stratigraphic model presented in Figure 5 can be examined for implications concerning the tectonic history of this area. The upper and lower reflectors dip at ~4.3° and ~5°, respectively, implying that a significant downwarping occurred which produced the regional dip

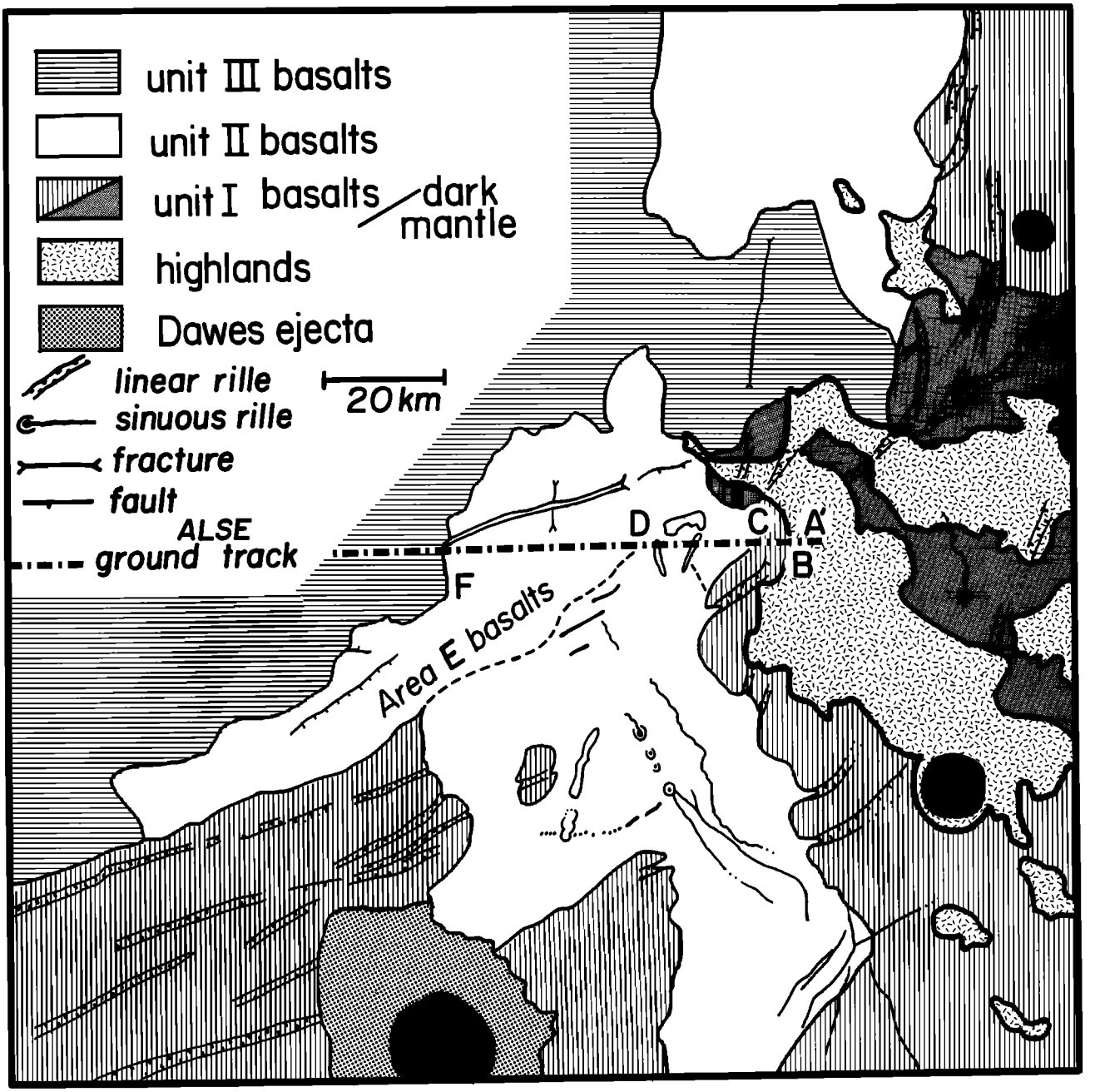

Fig. 4b

observed on the reflector surfaces. Furthermore, if the upper reflecting horizon, representing the unit II surface, is restored to its original horizontal configuration, the lower horizon (the unit I surface) slopes inward at only ~0.7°. Immediately after the emplacement of the unit II basalts, therefore, the unit I basalts had a modest inward slope of ~0.7°. According to the interpretation presented by *May et al.* [1976], *Maxwell* [1977], and *Phillips and Maxwell* [1978] then, it was not until after unit II was fully emplaced that the intense bending of the margins of Mare Serenitatis occurred. Surface observation reveals abundant evidence for a period of intense deformation which resulted not only in regional tilting of the mare surfaces but also produced numerous linear and arcuate graben trending primarily circumferential to the basin [*Howard et al.*, 1973; *Muehlberger*, 1974; *Solomon and Head*, 1979]. However, these graben are present only on unit I and highland surfaces. The graben do not transect the unit I/unit II boundary but are invariably truncated by the later unit II basalts (Figure 4). Thus surface observation clearly indicates that the episode of downwarping, which produced the graben and tilted the unit I surface, occurred prior to the emplacement of unit II, not after unit II, as the model in Figure 5 implies.

Thus reexamination of the interpretation presented in Figure 5 reveals several problems. In the following section, we recorrelate the surface and subsurface data sets and present an alternative model for the subsurface stratigraphy of Mare Serenitatis.

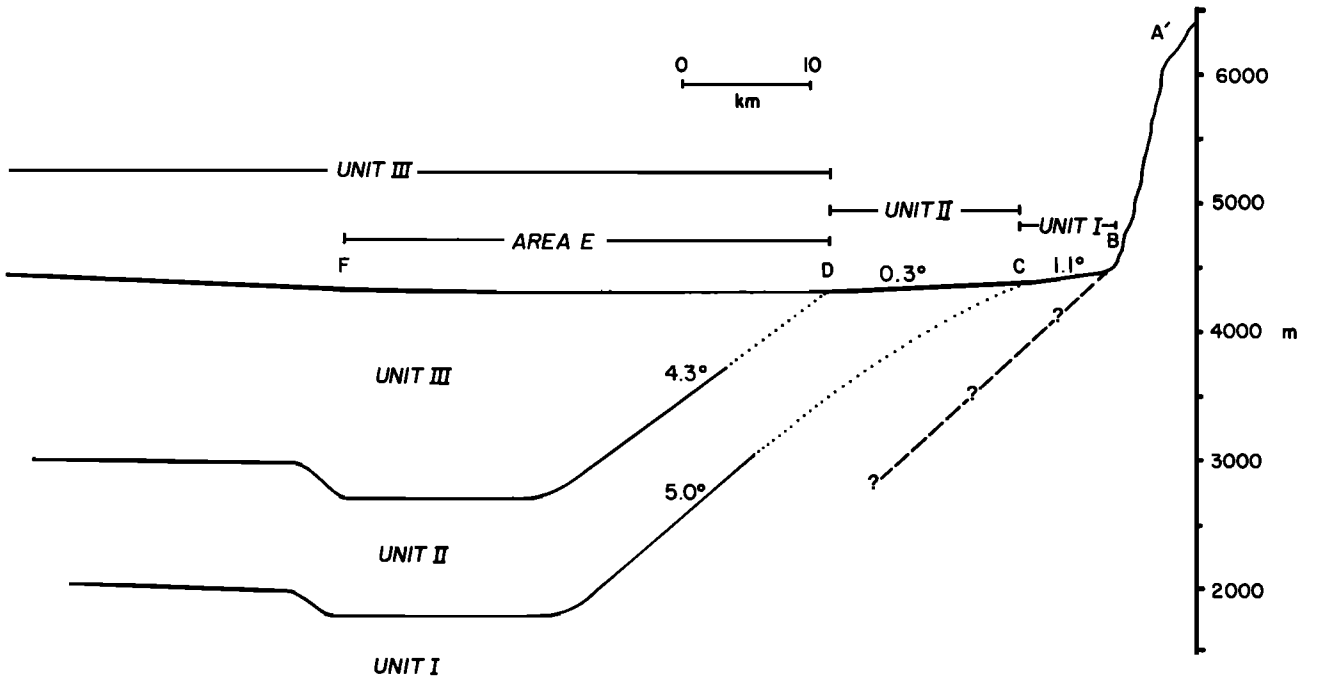

Fig. 5. Eastern portion of the ALSE profile shown in Figure 1 illustrating the stratigraphic model advanced by *May et al.* [1976] and others. This model relies upon surface unit relationships proposed by *Maxwell* [1977], which included the basaltic surface here labeled area E as a subunit of unit III. By a linear upward projection to point D, the upper subsurface horizon was interpreted as the unit III/unit II boundary. The lower subsurface horizon was correlated with point C, the unit II/unit I boundary. Subsurface horizons resolved by ALSE are depicted as solid lines; projections used by *May et al.* [1976] and others are dotted. Dashed line with (?) indicates the boundary between the unit I basalts and the highland material, which is not resolved in the ALSE data, according to their interpretation. The slope of relevant stratigraphic surfaces is shown above the respective surface. Letters A–F correlate with the plan view of Figure 4. Surface topography derived from LTO 43C3. See text for details.

Reinterpretation

On the basis of evidence presented below, we interpret the upper reflecting horizon to be the subsurface trace of the unit II/unit I boundary. The upper horizon joins with the unit II/unit I surface boundary at point C along a curved projection path, as shown in Figure 6. The lower horizon then projects to point B, the boundary between the unit I volcanics and the highland massif, Mons Argaeus. This assignment eliminates the need to have a regolith layer developed between unit II and the area E basalts, which appear to be contemporaneous subunits of the same episode of volcanism. In contrast, the boundary at point C, about 15 km east of the area E/unit II boundary (D, Figure 6), separates the older unit I volcanics, tilted at ~1.1°, from the younger unit II basalts, which slope westward at only ~0.3°. This discrete change in surface slope across the unit II/unit I boundary as well as the presence of numerous tectonic rilles which deform only the unit I and highland surfaces (Figure 4) record the occurrence of the extensive period of nondeposition between the emplacement of the unit I and unit II sequences that is required for regolith accumulation. In addition, the projection of the upper horizon can bend around to converge smoothly on the exposed unit I surface without the discrepancy in slope across the boundary that occurs when the upper horizon is projected to point D (Figure 5). The average slope of the curved projection to point C is ~2.1°, representing a decrease of ~2.2° over the slope measured from the upturned eastern end of the upper horizon (Figure 6). Examination of the reflecting horizons in the ALSE profile presented in Figure 1 illustrates that slope changes are characteristically effected along a broad, curved zone several kilometers wide, such as postulated here for the projection of the upper horizon (Figure 6), rather than simply intersecting to form an abrupt, angular inflection, such as results from the interpretation favored by *May et al.* [1976] and others (Figure 5). Finally, by correlating the upper horizon with the unit II/unit I boundary, the major episode of downwarping, inferred from the geometry of the subsurface reflecting horizons, occurred prior to the emplacement of the unit II basalts. Thus unlike the previous interpretation (Figure 5), the structural implications of the model favored here are consistent with surface evidence indicating major downwarping and faulting prior to the emplacement of unit II [*Howard et al.*, 1973; *Muehlberger*, 1974; *Solomon and Head*, 1979].

Nature of the Lower Reflector

The existence of the lower reflecting horizon across the Serenitatis basin implies the presence of a laterally extensive high-porosity layer at least ~2 m thick upon which the unit I basalts were emplaced. If this layer is developed on the surface of a post-Imbrium basin volcanic unit, then it would appear that the lower horizon, like the upper horizon, represents a regolith layer developed primarily by the long-term process of comminution and reworking by small-scale impacts. On the other hand, if the lower reflecting horizon is developed on a pre-Imbrium basin surface (either the basin floor or pre-existing volcanics), then ejecta deposited on this

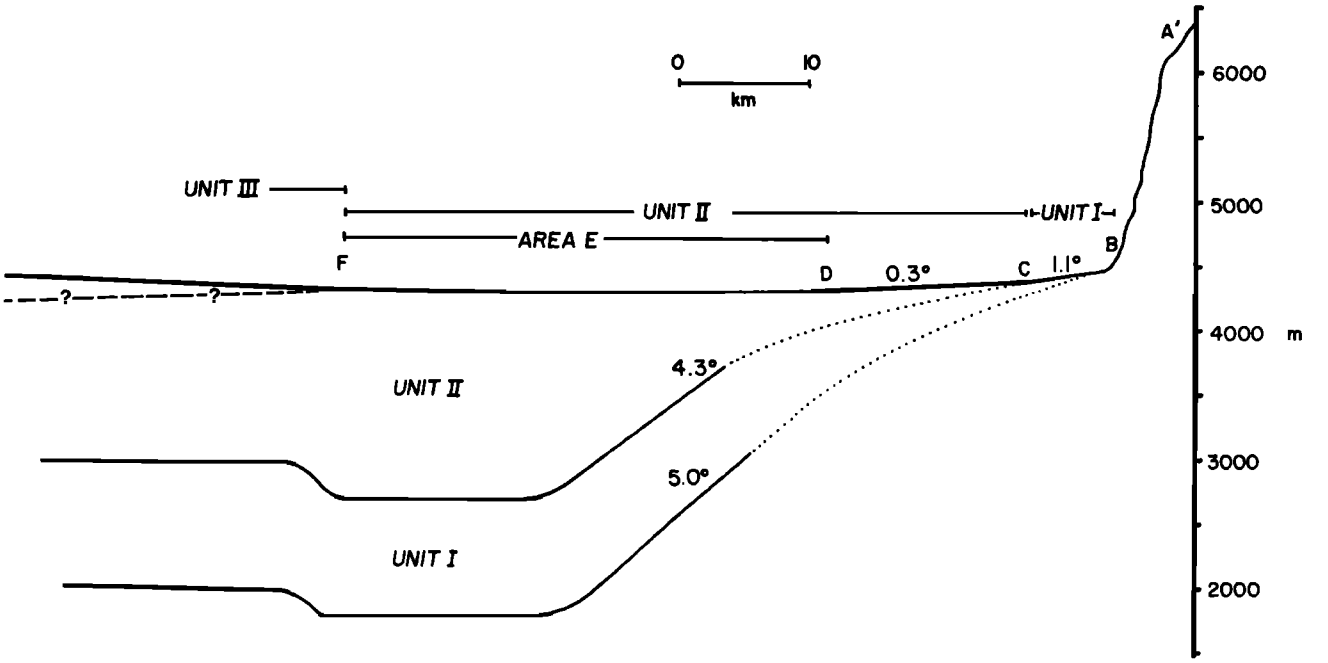

Fig. 6. Interpretation of the ALSE reflecting horizons proposed in this paper. Here the upper reflecting horizon represents the unit II/unit I boundary, and the lower reflecting horizon is the interface between the mare fill and the preexisting basin structure below. The unit III/unit II boundary (dashed line) does not appear in the ALSE data because of bandwidth limitations discussed in text.

surface by the Imbrium impact event could account for this high-porosity layer. Apollo 14 samples inferred to represent material 'reset' by the Imbrium event have Rb-Sr and ^{39}Ar–^{40}Ar ages which cluster around 3.80–3.82 b.y. [*Schaeffer and Schaeffer*, 1977; *Nyquist*, 1977]. Considering uncertainty ranges, these ages are virtually coincident with the oldest isotopic ages of Apollo 17 basalts [*Schaeffer and Schaeffer*, 1977; *Nyquist et al.*, 1975]. It therefore seems unlikely that a sufficient amount of time elapsed between the Imbrium event and commencement of unit I volcanism to accomplish the emplacement of a pre-unit I sequence of basalts and the development of an adequate regolith layer on top of this sequence. The more plausible explanation thus appears to be that the lower reflector represents the Fra Mauro Formation emplaced on top of the modified Serenitatis basin floor.

Pre-Imbrium Basin Units

While there is no apparent surface expression of a pre-Imbrium basin volcanic unit within Mare Serenitatis, the identity of such a unit could be obscured by Imbrium ejecta or subsequent volcanic activity. Surface observations, however, discussed in a later section imply that load-induced downwarping [*Solomon and Head*, 1979] did not begin until after the emplacement of unit I. Thus if the Serenitatis basin topography was compensated primarily by relief on the lunar Moho [*Wise and Yates*, 1970; *Head*, 1974] or other nonextrusive mechanisms [*Dvorak and Phillips*, 1979] prior to initiation of mare volcanism, then pre-Imbrium basin mare units are volumetrically negligible. Alternatively, if compensation of the Serenitatis basin was not completely achieved at the onset of mare volcanism, then some basalt fill would be required to achieve isostasy, with only later additions contributing to the downward load. Determination of the significance of precompensation basalts within Mare Serenitatis might be accomplished by comparing the predicted gravity field for the model we present herein with the available gravity data over Mare Serenitatis. We note that as the unit I basalts appear to have been emplaced prior to the onset of extensive downwarping and fracturing, a substantial fraction of unit I could be precompensation.

Shallow Units

On the basis of the interpretation developed thus far, a subsurface reflecting horizon representing the unit III/unit II interface does not appear in the radar profile. It is possible that the period of surface exposure between the termination of unit II volcanism and the onset of unit III volcanism was too brief to permit the development of a sufficiently thick regolith layer. Alternately, a regolith layer could have developed but is too shallowly buried (<400 m) to be resolved by the HF-1 experiment. Several lines of evidence appear to support the hypothesis that the unit III/unit II boundary is <400 m deep.

1. The crater Bobillier (6.5-km diameter) lying along the radar profile in western Serenitatis (Figure 1) has been partially flooded by the last sequence of mare basalts (unit III), as evidenced by the absence of a visible ejecta blanket around the crater. On the basis of reasonable assumptions for rim height/diameter ratios, *Young* [1977] calculated the depth to which Bobillier was flooded to be approximately 150–200 m.

2. *Young et al.* [1974] and *Young* [1975, 1977] have discussed anomalies in the size distributions, shapes, and ejecta characteristics of craters less than 1 km in diameter located in central Mare Serenitatis. They conclude that these unusual effects might be due to a regolith layer buried at a depth of ~50 m. This seems to indicate that at least in some areas of central Mare Serenitatis an appreciable regolith was developed on the unit II surface.

3. The stratigraphy exposed in the walls of Bessel Crater

(15.3-km diameter) north of the profile region also provides an indication of a shallow subsurface interface. The younger tan flows (unit III) of the central basin appear to be underlain at a depth of ~350 m by blue-gray flows similar in appearance to the older dark annulus flows (unit II?) which occur around the basin margin [*Young*, 1977]. The above observations all suggest that the unit II/unit III interface is shallow (50–350 m deep). On the basis of these data as well as the conspicuous absence of a reflecting horizon that is correlatable with the unit II/unit III boundary, it appears than the unit III volcanics are probably no thicker than ~400 m within Mare Serenitatis.

RECONSTRUCTION OF PALEOTOPOGRAPHY

The three stratigraphic surfaces depicted in the ALSE profile across Mare Serenitatis (Figure 7*a*) can be used to reconstruct the general configuration of the stratigraphy that existed, at two instances during the process of basin infilling.

Method

The highly fluid nature and high mass eruption rates characteristic of mare basalts have been documented through numerous photogeologic [e.g., *Schaber*, 1973; *Gifford and El Baz*, 1978], petrologic [*Brett*, 1975; *Murase and McBirney*, 1970], and theoretical [*Wilson and Head*, 1981] studies. These characteristics tend to support the assumption that the upper surface of mare units was initially near-planar and horizontal. It is presumed, therefore, that the present deviations from the horizontal (Figure 7*a*) represent deformation of this initial surface. The topography developed on the upper horizon, representing the upper surface of unit I, records the deformation that the lithosphere has incurred subsequent to the emplacement of volcanic unit I. By removing the amount of topographic relief developed on the upper reflecting horizon from the lower horizon, the lower horizon (which appears to be the modified pre-mare basin floor) is restored to its topographic state at the time unit I was emplaced (Figure 7*c*). The upper surface of unit II does not appear in the ALSE profile, as discussed previously; thus its configuration is uncertain. The structural effect following the emplacement of the unit III basalts is recorded, however, in the present surface topography. By subtracting this effect from the upper horizon, the unit I/unit II interface can be restored to its approximate appearance at the time of unit III emplacement (Figure 7*b*). The ALSE data therefore permit the direct reconstruction of two pieces of information in the history of Mare Serenitatis: (1) the basin topography as it appeared immediately after the emplacement of unit I (~3.75 b.y.) and (2) the unit I/unit II interface as it appeared immediately after the emplacement of unit III (~3.2 b.y.).

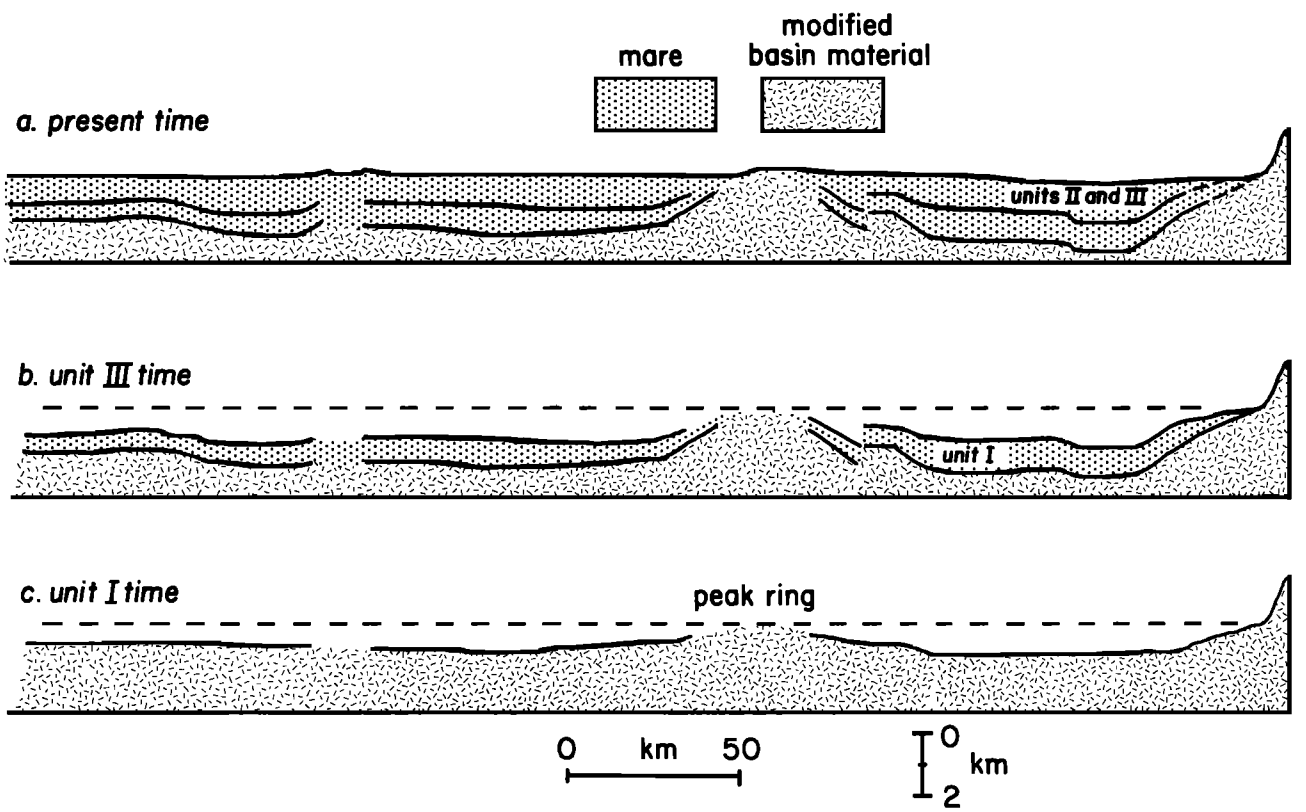

Fig. 7. (*a*) Present stratigraphic/topographic configuration of Mare Serenitatis along the eastern portion of ALSE ground track that results from correlating the subsurface radar horizons with surface boundaries, as shown in Figure 6. Where subsurface horizons (denoted by solid lines) are absent, results are interpreted on the basis of simple extrapolation. (*b*) Reconstruction of the configuration of the unit I surface immediately after emplacement of unit III (~3.2 b.y.), assuming that all topography on the present unit II surface resulted from postemplacement deformation. Dashed line represents the inferred undeformed unit III surface. (*c*) Reconstruction of the configuration of the pre-mare basin floor (modified by Imbrium ejecta) immediately after the emplacement of unit I. Dashed line represents the inferred undeformed unit I surface. Analysis of linear rilles around Mare Serenitatis suggests that major load-induced flexure did not occur until after unit I emplacement was complete. Thus Figure 7*c* represents a close approximation of the pre-mare Serenitatis basin topography. See text for details.

Pre-Unit I Basin Geometry

The basin topography, as it appeared immediately after the emplacement of unit I, is presented in Figure 7*c*. Does this reconstruction, however, represent an accurate approximation of the configuration of the Serenitatis basin (modified by Imbrium ejecta) before unit I was emplaced? We rely upon surface observations to ascertain the significance of the deformation that occurred during or prior to the emplacement of unit I. Examination of linear and arcuate rilles which deform the flanks of Serenitatis [*Lucchitta and Watkins*, 1978] uncovered no evidence to indicate that these rilles have been embayed or truncated by unit I volcanics. Thus if rille formation was caused by subsidence of the basin floor [*Bryan*, 1973; *Runcorn*, 1977] and associated flexure [*Solomon and Head*, 1980], this deformation began primarily after the majority of unit I volcanics had been emplaced. We conclude that the lithosphere of the basin floor did not deform appreciably during the emplacement of unit I. The basin geometry, as it appeared immediately after unit I emplacement (Figure 7*c*), is therefore probably an accurate approximation of the Serenitatis basin geometry immediately prior to the emplacement of unit I.

Radial Projection of the ALSE Data

The ALSE ground track did not pass through the center of the Serenitatis basin (Figure 3). The topographic gradients therefore are somewhat shallower than the true structural dips, assuming that the structural trends are concentric to the basin center. To approximate the true appearance of the topography (i.e., structure) sampled by ALSE, the profile is geometrically transformed into an idealized basin radial profile by the following technique. The basin center is approximated by determining the origin of the circle best fit by the concentric mare ridge ring, as shown by point O in Figure 8. From the origin, a radius is described which intersects the eastern terminus of the ALSE ground track (A′ in Figure 8). Each point along the ALSE profile is then projected onto the radius 0-A′ along arcs concentric to the basin center, as shown in Figure 8. The results of this radial transformation for the eastern portion of the ALSE profile and the interpreted pre-mare configuration are presented in Figure 9.

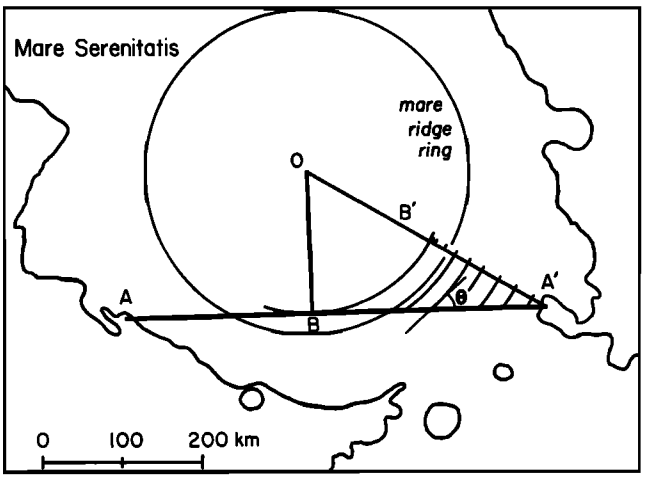

Fig. 8. Sketch map showing manner in which the idealized radial projection (A′–B′) was accomplished. Points along the eastern half of the ALSE profile were projected onto the radius O–A′ along arcs concentric to the basin center, O (~25°N latitude, 18.5°E longitude). Examples of the concentric projection paths for each degree of longitude along the ground track are shown as tick marks on line O–A′. The arcs intersect the ground track at angle θ, which decreases westward until at B, where $\theta = 0$. Point B then represents the closest approach of the ALSE ground track to the basin center, and point B′ is its radial projection. Zones of equal length along the ALSE ground track (such as degrees longitude) are projected onto the basin radius as zones which decrease in width toward the basin center.

DISCUSSION

Serenitatis Basin Geometry: Location of the Peak Ring

The most conspicuous feature of the pre-mare basin topography (Figures 7*c* and 9*b*) is the large topographic prominence in the eastern portion of the profile. Unit I is thinned on the flanks of the arch, as shown in Figure 9*a*, requiring that the arch existed at the time of unit I volcanism. Thus this arch appears to be related to the original basin geometry rather than a feature induced by (post-unit I) tectonic deformation or igneous intrusion, as suggested by *Maxwell et al.* [1975].

Head [1979] compared the premare interior basin topography of Serenitatis with the similarly sized Orientale basin. The results of this comparison indicate that the location of the prominent concentric system of mare ridges shown in Figure 1 corresponds to the location of the Inner Rook Mountains, interpreted as the peak ring structure in the unflooded Orientale basin [*Head*, 1974]. The topographic arch observed in Figure 7 lies directly beneath the eastern intersection of this ridge system and the ALSE ground track. Beneath the mare ridge system in the west the subsurface topography is not well defined because no reflecting horizons appear in the westernmost portion of the traverse. Examination of Figure 1, however, indicates that the basin surface (lower horizon) does slope sharply upward from the east near the ridge system, implying that another subsurface arch may be located beneath the western ridge intersection. The location of these subsurface arches beneath both intersections with the concentric mare ridge system suggests that the structural trend of the subsurface arch is also concentric. The radial projection of the ALSE profile (Figure 9) shows the true dip and true width of concentrically oriented topographic features along the eastern portion of the profile. The basin radial projection of the unit I topography (Figure 9*b*) was compared to the regional slope across the Orientale basin developed from earth-based limb profile photographs (Figure 10). Results indicate that the width (~50–75 km) and relief (~1.5 km) of the subsurface arch in Serenitatis are similar to the dimensions of the peak ring Inner Rook Mountains in Orientale. Thus the surface topography is consistent with the ring assignment of *Head* [1979], and thus we conclude that the subsurface arch apparent in the ALSE profile is the buried peak ring structure of the Serenitatis basin.

Thickness of Mare Fill

Several techniques have been devised to calculate the approximate thickness of the volcanic units within a mare basin including: (1) the morphometric analysis of flooded ('ghost') craters [e.g., *Baldwin*, 1970; *De Hon*, 1974, 1977, 1979; *De Hon and Waskom*, 1976; *Hörz*, 1978], (2) the morphometric analysis of post-mare craters which penetrate

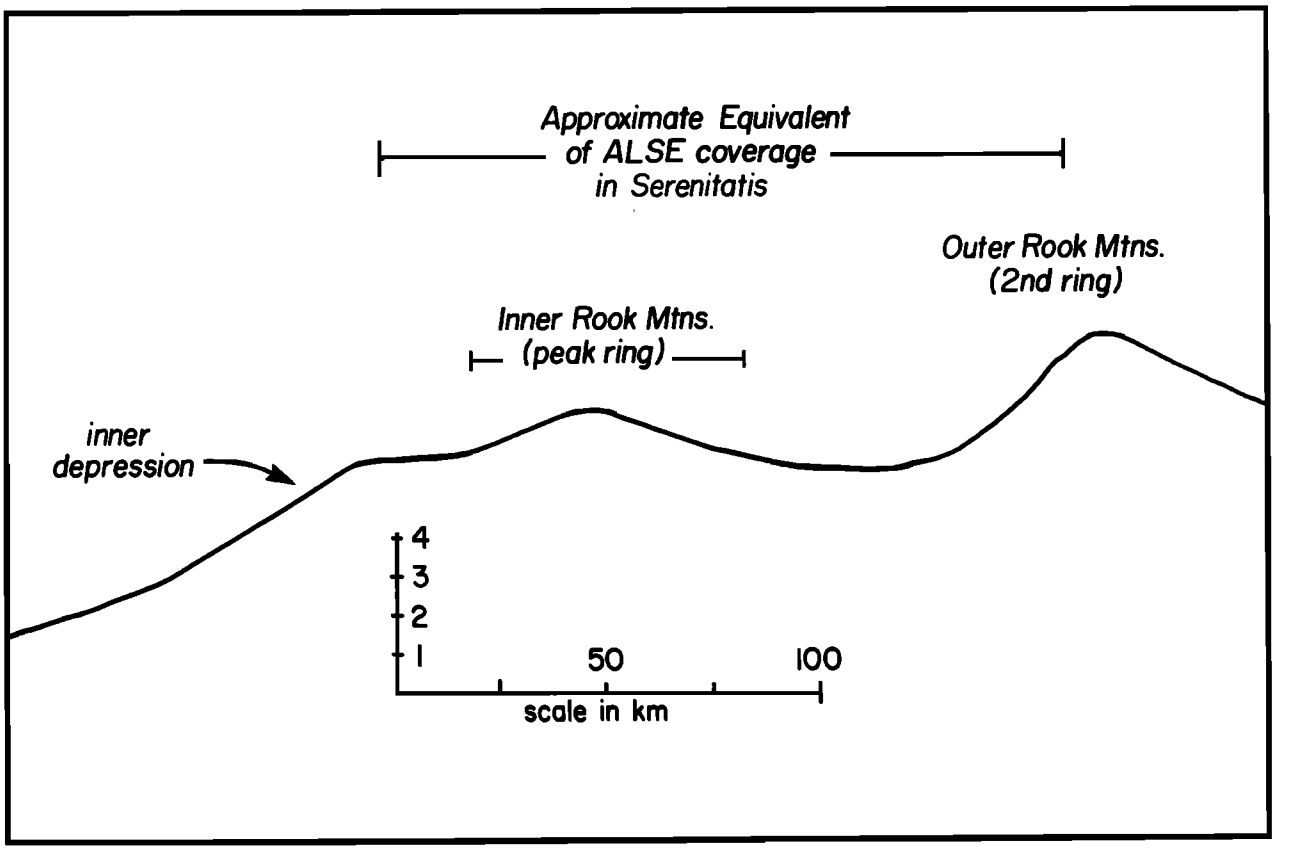

Fig. 9. Radial projection of the ALSE profile resulting from technique illustrated in Figure 8. Information presented in Figure 7*a* showing the present stratigraphic cross section is projected in Figure 9*a*. The pre-unit I configuration illustrated in Figure 7c is projected in Figure 9*b*. Horizontal scale shows the radial distance from basin center of each projection. Vertical scale is in increments of 1 km each.

the mare fill [e.g., *Head et al.*, 1978; *Andre et al.*, 1979], (3) the projection of surface gradients beneath the mare fill [e.g., *Head*, 1974], and (4) geophysical techniques such as gravity analysis [*Phillips et al.*, 1972; *Talwani et al.*, 1973] and seismic experiments [e.g., *Cooper et al.*, 1974]. These techniques, their inherent uncertainties, and related problems are discussed by *Head* [1982]. In contrast to the numerous indirect methods of deriving an estimate of the mare thickness listed above, the Serenitatis ALSE profile appears to provide the only direct measurement of basaltic thicknesses across a mare basin. Implicit to the thickness estimates that follow is the assumption that for that portion of the basin traversed by ALSE (i.e., the southern flank of Serenitatis) compensation was achieved prior to mare emplacement and therefore the depth to the lower reflecting horizon defines the thickness of the mare basalts in this region. The maximum total thickness of about 2.5 km along the ALSE ground track occurs within a narrow trough at the eastern end of the profile (Figure 9*a*). The average thickness of the mare basalts is ~1.6 km, although the thickness is extremely variable due to the effects of the pre-mare topography and local zones of concentrated deformation. For instance, the eastern peak ring structure appears to be buried by not more than 400 m of mare basalts, and interpolation of the lower reflector across the unresolved interval at the peak ring (Figure 7*c*) suggests that the mare is no more than a thin veneer in this area, perhaps only a few tens of meters thick. These thicknesses compare favorably with those derived by *Head* [1982] on the basis of a simulated lava flooding of the Archimedes-Apennine Bench region of Mare Imbrium.

Because the ALSE profile passes well south of the Serenitatis basin center, it effectively samples only the outer portion of the concentric basin structure (Figure 9). The inner unsampled region (~190 km, radius) could contain basalt accumulations much thicker than those observed. The topographic profile of Orientale (Figure 10) reveals that this basin exhibits a distinct topographic depression located about 50–60 km inside the peak-ring-related topography. There appears to be as much as 6 km of relief from the terrace above this inner depression to the basin floor below [*Head et al.*, 1981]. If a similar inner depression exists in the Serenitatis basin, it would lie beyond the range sampled by ALSE. Thus it is likely that the maximum depth of volcanic fill within Mare Serenitatis significantly exceeds the maximum depth detected along the ALSE profile (Figure 9*a*).

Gravity Implications

Recent theories of origin for the positive gravity anomalies ('mascons') associated with lunar circular mare basins have included deep subsurface effects such as updoming of the crust-mantle interface [*Wise and Yates*, 1970; *Head*, 1974; *Bowin et al.*, 1975; *Sjogren and Smith*, 1976] and near-surface effects such as superisostatic volcanic loading [*Wood*, 1970; *Phillips et al.*, 1972; *Sjogren et al.*, 1972, 1974]. *Phillips et al.* [1972] and *Muller et al.* [1974] have shown that by assuming a simple disc shaped model, a superisostatic

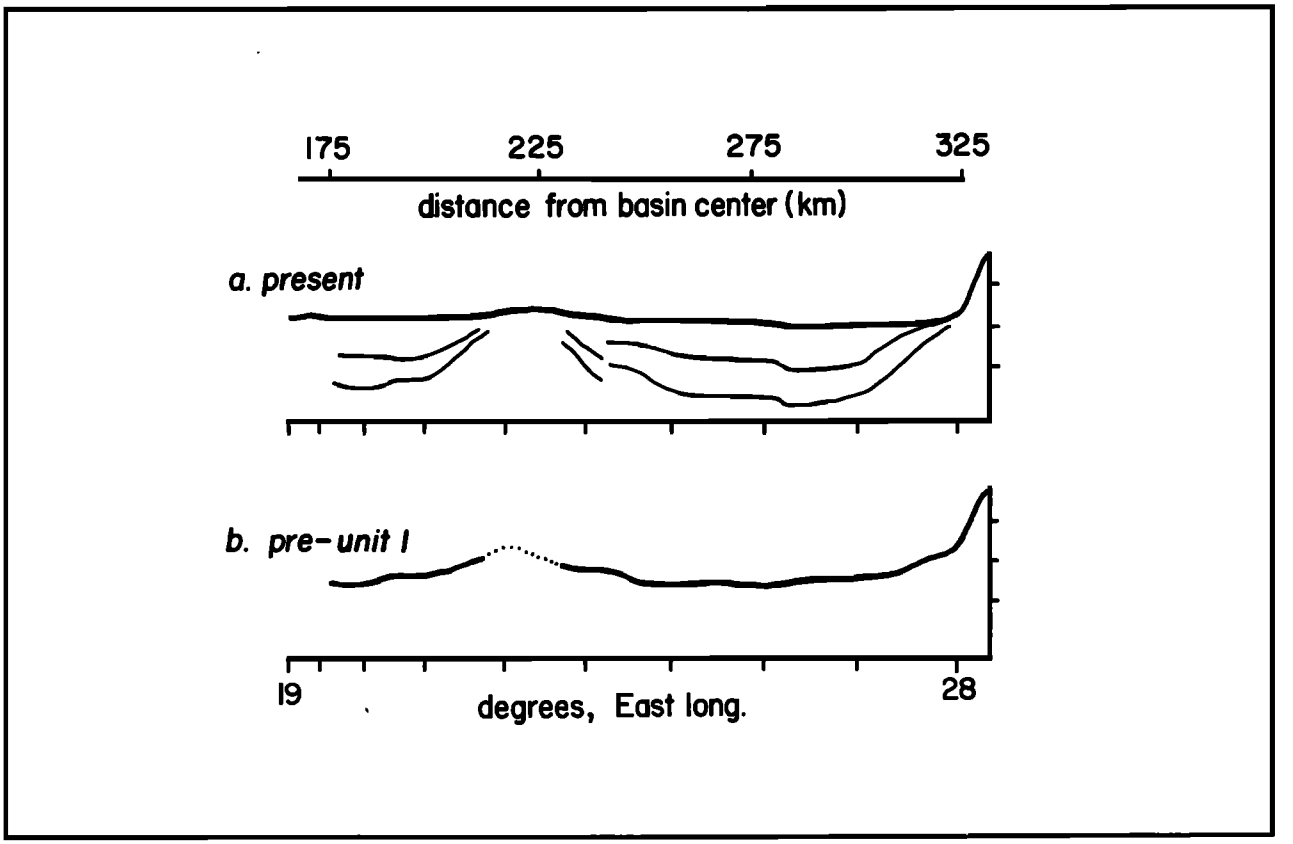

Fig. 10. Regional topography of the Orientale basin shown to same (vertical and horizontal) scale as Figure 9. The spacing and dimensions of the peak ring in Serenitatis (Fig. 9b) are comparable to the Inner Rook Mountains in Orientale. A distinct steepening in slope (inner depression) occurs ~50 km inside the Orientale peak ring. A similar feature, if it exists in Serenitatis, would be unsampled by the ALSE traverse. Adapted from *Solomon and Head* [1979].

surface load is one solution that adequately accounts for the observed gravity anomaly across Mare Serenitatis. This model implies a sharp increase in load thickness at the concentric mare ridge ring (~240–245 km radius; *Phillips et al.* [1972]), a uniform load thickness of 2.5–3 km across the interior of the basin [*Phillips et al.*, 1972; *Muller et al.*, 1974] and disregards any excess mass distributed outside the mare ridge ring. *Sjogren et al.* [1974] have since shown that a surface disc of smaller radius (221 km) provides a better fit to the Apollo 17 gravity data.

The stratigraphic model presented herein indicates that the distribution of mare fill within the Serenitatis basin is controlled by pre-mare topography and therefore the thicknesses are highly variable across the portion of the basin traversed by ALSE. There is no indication of a sharp increase in basalt thickness at the mare ridge ring, although by analogy with Orientale, a steep and substantial increase, located ~50 km inside the peak ring, is suggested. Substantial amounts of fill (~2.5 km, maximum) accumulated outside the mare ridge ring in the depression between the basin ring structures of southeastern Serenitatis.

The downwarped upper surface of unit I (Figure 9*a*), however, implies that this unit is at least partially compensated; the thickness of the superisostatic fill (i.e., the present load) is therefore somewhat less than the total mare thickness measured from the ALSE profile. Hypothetically, the volcanic fill in the region sampled by ALSE (particularly the basalts outside the mare ridge ring) could be virtually compensated. The gravity anomaly may then result from the deep accumulations of basalt which could lie just beyond the innermost region sampled by ALSE.

Alternatively, the fill thickness detected by ALSE (Figure 9*a*) may approximate the load thickness, i.e., compensation of the detected basalts was minimal. This would imply that the actual load geometry is more complicated than the simple disc models would suggest. Determination of the relative significance of this hypothesis awaits gravity analyses using more complex load models.

Structural Implications

Along the ALSE traverse in southeastern Serenitatis the earliest sequence of mare basalts (unit I) accumulated to a maximum depth of ~1.2 km within the intra-ring depressions of the modified basin topography. However, topographic highs associated with the basin ring structures were only thinly flooded or remained unflooded. This variable distribution of the unit I load initiated a nonuniform tectonic response: thinly flooded regions underwent nominal subsidence (<400 m) compared to the more deeply flooded regions between the rings which show as much as 1.7 km of subsidence. Tensional and bending stresses associated with this differential movement developed along the flanks of the high standing topography. This resulted in the formation of the more or less concentric network of linear and arcuate graben (rilles) observed along the margins of the basin (Figure 4).

The reconstruction presented in Figure 7*b* illustrates that the tectonic response that resulted in rille development along the margins of the basin also produced several local zones of differential movement:

1. A narrow trough ~25 km across developed at the base of the slope extending upward to Mons Argaeus [*Maxwell*, 1977]. This trough appears to have subsided ~300 m more than the adjacent area. A shallow depression ~100 m deep, 30 km wide, and 100 km long, is developed on the present mare surface directly above this trough. Although the surface depression is developed on unit II basalts, it probably originated after the emplacement of unit III, or it would have been filled or embayed by the last stages of volcanism. Thus while subsidence of the trough was greatest prior to the emplacement of unit III, surface expression indicates that this feature continued to subside after unit III emplacement.
2. A vertical offset in the reflecting surfaces is observed just east of the peak ring; the offset is ~300 m with the western side displaced downward. This feature is surficially characterized by a small, poorly developed mare ridge, less than 100 m in relief.
3. A zone of intense disruption of the reflecting horizons ~15 km across is located about midway across the profile (Figure 1). The margins of this zone appear upturned, although the resolution of the central portion of this zone is obscured, perhaps due to surface scatter from the two en echelon mare ridges located on the unit III surface above the disrupted zone. The cross-sectional shape of the ridges appears to be similar to the shape of the subsurface feature. The magnitude of the relief across the ridges, however, is less than that of the subsurface feature. This implies that this feature, like the previous two, continued to develop throughout the history of mare emplacement but that most deformation occurred prior to the emplacement of unit III. These features could be associated with (1) zones of weakness related to the basin-forming event which were reactivated during volcanic loading, (2) structural heterogeneities in the lithosphere that predate the formation of the basin, or (3) localized zones of weakness caused by variations in local load thicknesses.

Comparison of Figures 7*a* and 7*b* shows that very little deformation took place after the emplacement of unit III. The maximum structural relief across the ALSE ground track that is attributable to post-unit III time is ~600 m. As unit III is constrained to be <400 m thick, some of the structural relief developed after the emplacement of unit III must have resulted from the remaining load of earlier volcanics.

Four mare ridge systems are transected by the ALSE profile (Figure 1). The concurrence of all mare ridges with anomalies in the subsurface horizons such as vertical displacements, disruptions, or topographic arches implies that these ridges are related to tectonic deformation associated with volcanic loading [*Sharpton and Head*, 1981].

CONCLUSIONS

The subsurface radar-reflecting horizons observed in the ALSE traverse across Mare Serenitatis are directly correlatable with the major episodes of volcanic infilling of the basin. The lower horizon is interpreted to be the interface between the earliest known volcanic episode in the region, unit I, and the fractured and modified pre-mare materials below. The upper reflecting horizon represents the regolith developed on the surface of the earliest unit (unit I; ~3.8 b.y.) during an extended period of exposure to impact processes prior to burial by subsequent volcanics (unit II; ~3.5 b.y.). The interface between the unit II basalts and the youngest unit (unit III; ~3.2 b.y.) is not evident on the ALSE traverse because unit III is less than 400 m thick and thus undetectable by the experiment.

From the three-dimensional structural and stratigraphic framework that results from this correlation and additional surface observations presented herein, we derive the following conclusions:

1. The history of volcanic infilling of Mare Serenitatis was characterized by three major episodes of volcanism. The upper subsurface horizon, representing a ≥2-m-thick accumulation of regolith, implies an extended period of time (of the order of 10^8 years) elapsed between the culmination of unit I volcanism and the onset of unit II volcanism.
2. The depth of volcanic fill within Serenitatis is highly variable; the average thickness of mare basalts under the ALSE ground track is ~1.6 km. The maximum depth observed along the ALSE traverse, located along the southern edge of the Serenitatis basin, is ~2.5 km. Comparison with the Orientale basin topography suggests that a major increase in load thickness could occur a few kilometers basinward of the innermost extent of the traverse.
3. The large archlike feature in the subsurface at the intersection of the ALSE traverse and the concentric mare ridge system existed as a major topographic feature prior to the onset of mare volcanism. This precludes an origin for this feature through tectonic processes or volcanic intrusion. The height (~1.3 km) and true width (~75 km) are comparable to the dimensions of the peak ring structure of the Orientale basin.
4. Primary basin-related topography exerted a major influence throughout the volcanic and tectonic modification of southern Mare Serenitatis.
5. The majority of deformation occurred subsequent to unit I emplacement but prior to the emplacement of unit III. This period of deformation resulted in extensional faulting (prior to unit II) at the margins of the basin and faulting, buckling, and differential subsidence in the more deeply flooded areas. Zones of weakness activated during this early episode of downwarping were reactivated during subsequent deformation episodes.
6. The latest volcanic episode (unit III; ~3.2 b.y.) resulted in an extensive but thin (<400 m) basaltic unit. The maximum structural relief that occurred after the emplacement of unit III, however, is ~600 m, suggesting that the lithosphere was continuing to adjust to the volcanic load of units II and I beyond the time unit III was emplaced.
7. The association of all mare ridges transected by the ALSE ground track with distinct offsets or depth changes in the subsurface layering indicates that these surface features are tectonic in origin.

Acknowledgments. We gratefully acknowledge the assistance of Susan Sharpton (typing), Angel Hilliard (proofing), Gwen Winston (drafting), and Sam Merrell (photography) in manuscript preparation. Valuable discussions and correspondence with Roger Phillips, Ted Maxwell, Peter Mouginis-Mark, Richard Grieve, Stan Zisk, Keith Howard, and Sean Solomon are greatly appreciated. We also thank Richard Young and Paul Spudis for constructive reviews of the manuscript. This work was supported by National Aeronautics and Space Administration grant NGR-40-002-088 from the Planetary Geology Program. One of us (V.L.S.) was supported by a fellowship from the William F. Marlar Foundation.

REFERENCES

Adams, J. B., C. Pieters, and T. B. McCord, Orange glass: Evidence of regional deposits of pyroclastic origin on the moon, *Proc. Lunar Sci. Conf., 5th*, 171–186, 1974.

Andre, C. G., R. W. Wolfe, I. Adler, and P. E. Clark, Mare basalt depths from orbital x-ray data, *Lunar Planet. Sci., X*, 38–40, 1979.

Baldwin, R. B., A new method of determining the depth of lava in lunar maria, *Publ. Astron. Soc. Pac., 82*, 857–864, 1970.

Bowin, C., B. Simon, and W. R. Wollenhaupt, Mascons—A two body solution, *J. Geophys. Res., 80*, 4955–4964, 1975.

Boyce, J. M., Ages of flow units in lunar nearside maria based on Lunar Orbiter IV photographs, *Proc. Lunar Sci. Conf., 7th*, 2717–2728, 1976.

Bratt, S. R., S. C. Solomon, and J. W. Head, Evolution of multi-ringed basins: Cooling, subsidence and thermal stress, *Lunar Planet. Sci., XII*, 109–111, 1981.

Brett, R., Thickness of some lunar mare basalt flows and ejecta blankets based on chemical kinetic data, *Geochim. Cosmochim. Acta, 39*, 1135–1141, 1975.

Bryan, W. B., Wrinkle ridges and deformed surface crust on ponded mare lava, *Proc. Lunar Sci. Conf., 4th*, 93–106, 1973.

Cooper, M. R., R. L. Kovach, and J. S. Watkins, Lunar near-surface structure, *Rev. Geophys. Space Phys., 12*, 291–308, 1974.

De Hon, R. A., Thickness of mare material in the Tranquillitatis and Nectaris basins, *Proc. Lunar Sci. Conf., 5th*, 53–59, 1974.

De Hon, R. A., Mare Humorum and Mare Nubium: Basalt thickness and basin-forming history, *Proc. Lunar Sci. Conf., 8th*, 633–641, 1977.

De Hon, R. A., Structural model of the Imbrium basin, *Lunar Planet. Sci., X*, 271–273, 1979.

De Hon, R. A., and J. D. Waskom, Geologic structure of the eastern mare basins, *Proc. Lunar Sci. Conf., 7th*, 2729–2746, 1976.

Dvorak, J., and R. J. Phillips, Gravity anomaly and structure associated with the Lamont region of the Moon, *Proc. Lunar Planet. Sci. Conf., 10th*, 2265–2275, 1979.

Geiss, J., P. Eberhardt, N. Grögler, S. Guggisberg, P. Maurer, and A. Stettler, Absolute time scale of lunar mare formation and filling, *Philos. Trans. R. Soc. London, Ser. A, 285*, 151–158, 1977.

Gifford, A. W., and F. El-Baz, Thickness of mare flow fronts, *Lunar Planet. Sci., IX*, 382–384, 1978.

Hartmann, W. K., Early lunar cratering, *Icarus, 5*, 406–418, 1966.

Hartmann, W. K., Preliminary note on lunar cratering rates and absolute timescales, *Icarus, 12*, 131–133, 1970*a*.

Hartmann, W. K., Lunar cratering chronology, *Icarus, 13*, 299–301, 1970*b*.

Hartmann, W. K., Paleocratering of the moon: Review of post-Apollo data, *Astrophys. Space Sci., 17*, 48–64, 1972.

Head, J. W., Orientale multi-ringed basin interior and implications for the petrogenesis of lunar highland samples, *Moon, 11*, 327–356, 1974.

Head, J. W., Serenitatis multi-ringed basin: Regional geology and basin ring interpretation, *Moon Planets, 21*, 439–462, 1979.

Head, J. W., Lava flooding of ancient planetary crusts: Geometry, thickness, and volumes of flooded lunar impact basins. *Moon Planets, 26*, 61–88, 1982.

Head, J. W., J. Adams, T. McCord, C. Pieters, and S. Zisk, Regional stratigraphy and geologic history of Mare Crisium, in *Mare Crisium: The view From Luna 24*, edited by R. B. Merrill and J. J. Papike, pp. 43–74, Pergamon, New York, 1978.

Head, J. W., E. Robinson and R. J. Phillips, Topography of the Orientale basin, *Lunar Planet. Sci., XII*, 421–423, 1981.

Hintenberger, H., and H. W. Weber, Trapped gases in lunar fines and breccias, *Proc. Lunar Sci. Conf., 4th*, 2003–2019, 1973.

Hörz, F., Impact cratering and regolith dynamics, *Phys. Chem. Earth, 10*, 3–15, 1977.

Hörz, F., How thick are lunar mare basalts?, *Proc. Lunar Planet. Sci. Conf., 9th*, 3311–3331, 1978.

Howard, K. A., M. H. Carr, and W. R. Muehlberger, Basalt stratigraphy of southern Mare Serenitatis, Apollo 17 Preliminary Science Report, *NASA Spec. Publ., SP-330*, 29-1–29-12, 1973.

Huneke, J. C., E. K. Jessberger, F. A. Podosek, and G. J. Wasserburg, $^{40}AR/^{39}AR$ measurements in Apollo 16 and 17 samples and the chronology of metamorphic and volcanic activity in the Taurus-Littrow region, *Proc. Lunar Sci. Conf., 4th*, 1725–1756, 1973.

Husain, L., and O. A. Schaeffer, Lunar volcanism: Age of the glass in the Apollo 17 orange soil, *Science, 180*, 1353–1360, 1973.

Johnson, T. V., D. L. Matson, R. J. Phillips, and R. S. Saunders, Vidicon spectral imaging: Color enhancement and digital maps, *Proc. Lunar Sci. Conf., 6th*, 2677–2688, 1975.

Kuckes, A. F., Strength and rigidity of the elastic lunar lithosphere and implications for present-day mantle convection in the moon, *Phys. Earth Planet. Inter., 14*, 1–12, 1977.

Lucchitta, B. K., Geologic setting of the dark mantling material in the Taurus-Littrow region of the moon, Apollo 17 Preliminary Science Report, *NASA Spec. Publ., SP-330*, 29-13–29-25, 1973.

Lucchitta, B. K., Mare ridges and related highland scarps—Result of vertical tectonism?, *Proc. Lunar Sci. Conf., 7th*, 2761–2782, 1976.

Lucchitta, B. K., Topography, structure, and mare ridges in southern Mare Imbrium and northern Oceanus Procellarum, *Proc. Lunar Sci. Conf., 8th*, 2691–2703, 1977.

Lucchitta, B. K., and H. H. Schmitt, Orange material in the Sulpicius Gallus Formation at the southwestern edge of Mare Serenitatis, *Proc. Lunar Sci. Conf., 5th*, 223–234, 1974.

Lucchitta, B. K., and J. A. Watkins, Age of graben systems on the moon, *Proc. Lunar Planet. Sci. Conf., 9th*, 3459–3472, 1978.

MacDonald, G. J. F., Stress history of the moon, *Planet. Space Sci., 2*, 249–255, 1960.

Maxwell, T. A., Stratigraphy and tectonics of southeastern Serenitatis, Ph.D. thesis, 132 pp., Univ. of Utah, Salt Lake City, 1977.

Maxwell, T. A., Origin of multi-ring basin ridge systems: An upper limit to elastic deformation based on a finite-element model, *Proc. Lunar Planet. Sci. Conf., 9th*, 3541–3559, 1978.

Maxwell, T. A., F. El-Baz, and S. H. Ward, Distribution, morphology and origin of ridges and arches in Mare Serenitatis, *Geol. Soc. Am. Bull., 86*, 1273–1278, 1975.

May, T. W., W. J. Peeples, T. Maxwell, W. R. Sill, S. H. Ward, R. J. Phillips, R. Jordon, and E. Abbott, Subsurface layering in Maria Serenitatis and Crisium: Apollo Lunar Sounder Results, *Lunar Sci., VII*, 540–542, 1976.

Melosh, H. J., The tectonics of mascon loading, *Proc. Lunar Planet. Sci. Conf., 9th*, 3513–3523, 1978.

Muehlberger, W. R., Structural history of southeastern Mare Serenitatis and adjacent highlands, *Proc. Lunar Sci. Conf., 5th*, 101–110, 1974.

Muehlberger, W. R., Comparison of structural style between northern Mare Tranquillitatis and southern Mare Serenitatis, *Lunar Sci., VIII*, 694–696, 1977.

Muller, P. M., W. L. Sjogren, and W. R. Wollenhaupt, Lunar gravity: Apollo 15 Doppler radio tracking, *Moon, 10*, 195–205, 1974.

Murase, T., and A. R. McBirney, Viscosity of lunar lavas, *Science, 167*, 1491–1493, 1970.

Neukum, G., B. König, and J. Arkani-Hamed, A study of lunar impact crater size distributions, *Moon, 12*, 201–229, 1975.

Nyquist, L. E., Lunar Rb-Sr chronology, *Phys. Chem. Earth, 10*, 103–142, 1977.

Nyquist, L. E., B. M. Bansal, and H. Wiesmann, Rb-Sr ages and initial $^{87}Sr/^{86}Sr$ for Apollo 17 basalts and KREEP basalt 15386, *Proc. Lunar Sci. Conf., 6th*, 1445–1465, 1975.

Oberbeck, V. R., and W. L. Quaide, Genetic implications of lunar regolith thickness variations, *Icarus, 9*, 446–465, 1968.

Peeples, W. J., W. R. Sill, T. W. May, S. H. Ward, R. J. Phillips, R. L. Jordan, E. A. Abbott, and T. J. Killpack, Orbital radar evidence for lunar subsurface layering in Maria Serenitatis and Crisium, *J. Geophys. Res., 83*, 3459–3470, 1978.

Phillips, R. J. and T. A. Maxwell, Lunar sounder revisited: Stratigraphic correlations and structural inferences, *Lunar Planet. Sci., IX*, 890–892, 1978.

Phillips, R. J., J. E. Conel, E. A. Abbott, W. L. Sjogren, and J. B. Morton, Mascons: Progress toward a unique solution for mass distribution, *J. Geophys. Res., 77*, 7106–7114, 1972.

Phillips, R. J., G. F. Adams, W. E. Brown, Jr., R. E. Eggleton, P. Jackson, R. Jordan, W. I. Linlor, W. J. Peeples, L. J. Porcello, J. Ryu, G. Schaber, W. R. Sill, T. W. Thompson, S. H. Ward, and J. S. Zelenka, Apollo Lunar Sounder Experiment, Apollo 17 Preliminary Science Report, *NASA Spec. Publ., SP-330*, 22-1–22-26, 1973*a*.

Phillips, R. J., G. F. Adams, W. E. Brown, R. E. Eggleton, P. Jackson, R. Jordan, W. J. Peeples, L. J. Porcello, J. Ryu G. Schaber, W. R. Sill, T. W. Thompson, S. H. Ward, and J. S. Zelenka, The Apollo 17 Lunar Sounder, *Proc. Lunar Sci. Conf., 4th*, 2821–2831, 1973*b*.

Pieters, C. M., Mare basalt types on the front side of the Moon: A summary of spectral reflectance data, *Proc. Lunar Planet. Sci. Conf., 9th*, 2825–2849, 1978.

Porcello, L. J., R. L. Jordan, J. S. Zelenka, G. F. Adams, R. J. Phillips, W. E. Brown, S. H. Ward, and P. L. Jackson, The Apollo Lunar Sounder Radar System, *Proc. IEEE, 62*, 769–783, 1974.

Quaide, W. L., and V. R. Oberbeck, Development of the mare regolith: Some model considerations, *Moon, 13*, 27–55, 1975.

Runcorn, S. K., Early melting of the moon, *Proc. Lunar Sci. Conf., 8th*, 463–469, 1977.

Schaber, G. G., Lava flows in Mare Imbrium: Geological evaluation from Apollo orbital photography, *Proc. Lunar Sci. Conf., 4th*, 73–92, 1973.

Schaeffer, G. A., and B. A. Schaeffer, $^{39}Ar-^{40}Ar$ ages of lunar rocks, *Proc. Lunar Sci. Conf., 8th*, 2253–2300, 1977.

Scott, D. H., J. A. Watkins, and J. M. Diaz, Regional deformation of mare surfaces, *Proc. Lunar Planet. Sci. Conf., 9th*, 3527–3539, 1978.

Sharpton, V. L., and J. W. Head, Lunar mare arches and ridges: Relation of ridge lobes to small pre-existing craters, *Lunar Planet. Sci., XI*, 1024–1026, 1980.

Sharpton, V. L., and J. W. Head, The origin of mare ridges: Evidence from basalt stratigraphy and substructure in Mare Serenitatis, *Lunar Planet. Sci., XII*, 961–963, 1981.

Sjogren, W. L., and J. C. Smith, Quantitative mass distribution models for Mare Orientale, *Proc. Lunar Sci. Conf., 7th*, 2639–2648, 1976.

Sjogren, W. L., P. Gottlieb, P. M. Muller, and W. Wollenhaupt, Lunar gravity via Apollo 14 Doppler radio tracking, *Science, 175*, 165–168, 1972.

Sjogren, W. L., R. N. Wimberly, and W. R. Wollenhaupt, Lunar gravity: Apollo 17, *Moon, 11*, 41–52, 1974.

Solomon, S. C., The relationship between crustal tectonics and internal evolution in the moon and Mercury, *Phys. Earth Planet. Inter., 15*, 135–145, 1977.

Solomon, S. C., and J. Chaiken, Thermal expansion and thermal stress in the moon and terrestrial planets: Clues to early thermal history, *Proc. Lunar Sci. Conf., 7th*, 3229–3243, 1976.

Solomon, S. C., and J. W. Head, Vertical movement in mare basins: Relation to mare emplacement, basin tectonics and lunar thermal history, *J. Geophys. Res., 84*, 1667–1682, 1979.

Solomon, S. C., and J. W. Head, Lunar mascon basins: Lava flooding, tectonics, and evolution of the lithosphere, *Rev. Geophys. Space Phys., 18*, 107–141, 1980.

Talwani, M., G. Thompson, B. Dent, H. G. Kahle, and S. Buck, Traverse gravimeter experiment, Apollo 17 Preliminary Science Report, *NASA Spec. Publ., SP-330*, 13-1–13-13, 1973.

Tatsumoto, M., P. D. Nunes, R. J. Knight, C. E. Hedge, and D. M. Unruh, U-Th-Pb, Rb-Sr, and K measurements of two Apollo 17 samples, *Eos Trans. AGU, 54*, 614–615, 1973.

Thompson, T. W., K. A. Howard, R. W. Shorthill, G. L. Tyler, S. H. Zisk, E. A. Whitaker, G. G. Schaber, and H. J. Moore, Remote sensing of Mare Serenitatis, Apollo 17 Preliminary Science Report, *NASA Spec. Publ., SP-330*, 33-3–33-10, 1973.

Turner, G., P. H. Cadogan, and C. J. Yonge, Argon selenochronology, *Proc. Lunar Sci. Conf., 4th*, 1889–1914, 1973.

Wasserburg, G. J., D. A. Papanastassiou, F. Tera, and J. C. Huneke, Outline of lunar chronology, *Philos. Trans. R. Soc. London, Ser. A, 285*, 7–22, 1977.

Wilson, L., and J. W. Head, Ascent and eruption of basaltic magma on the earth and moon, *J. Geophys. Res., 86*, 2971–3001, 1981.

Wise, D. U., and M. T. Yates, Mascons as structural relief on a lunar 'Moho,' *J. Geophys. Res., 75*, 261–268, 1970.

Wood, J. A., Petrology of the lunar soil and geophysical implications, *J. Geophys. Res., 75*, 6497–6513, 1970.

Young, R. A., Mare crater size-frequency distributions: Implications for relative surface ages and regolith development, *Proc. Lunar Sci. Conf., 6th*, 2645–2662, 1975.

Young, R. A., A stratigraphic model for Bessel Crater and southern Mare Serenitatis, in *Impact and Explosion Cratering*, edited by D. J. Roddy, R. O. Pepin, and R. B. Merrill, pp. 527–538, Pergamon, New York, 1977.

Young, R. A., W. J. Brennan, and D. J. Nichols, Problems in the interpretation of lunar mare stratigraphy and relative ages indicated by ejecta from small impact craters, *Proc. Lunar Sci. Conf., 5th*, 159–170, 1974.

Zisk, S. H., G. H. Pettengill, and G. W. Catuna, High resolution radar maps of the lunar surface at 3.8 cm wavelength, *Moon, 10*, 17–50, 1973.

(Received April 29, 1982;
revised September 27, 1982;
accepted October 4, 1982.)